Donor-band ferromagnetism in cobalt-doped indium oxide

A. M. H. R. Hakimi* and M. G. Blamire
Department of Materials Science and Metallurgy, University of Cambridge, Pembroke Street, Cambridge CB2 3QZ, United Kingdom

S. M. Heald
Advanced Photon Source, Argonne National Laboratory, Argonne, Illinois 60439, USA

Marzook S. Alshammari, M. S. Alqahtani, D. S. Score, H. J. Blythe, A. M. Fox, and G. A. Gehring†
Department of Physics and Astronomy, Hicks Building, University of Sheffield, Sheffield S3 7RH, United Kingdom
(Received 21 April 2011; revised manuscript received 2 July 2011; published 18 August 2011)

Ferromagnetic cobalt-doped indium oxide, $(In_{1-x}Co_x)_2O_3$, thin films with x between 1.6% and 8.1% have been studied by x-ray, magnetic, and optical methods. Evidence gathered from x-ray diffraction and x-ray absorption fine-structure studies suggest that the Co atoms are substitutional within the In_2O_3 matrix. The magnetization of the films were found to consist of two components: a paramagnetic term that agrees with what is expected for paramagnetic cobalt ions and a temperature-dependent ferromagnetic hysteresis loop. The ferromagnetic component was too large to have been generated by the free carriers, implying that it originates from electrons bound in defect states associated with oxygen vacancies. This is confirmed by optical absorption and magneto-optical studies because the magnetic circular dichroism scales with concentration of cobalt and temperature in the same way as the measured magnetization.

DOI: 10.1103/PhysRevB.84.085201 PACS number(s): 78.20.Ls

I. INTRODUCTION

Dilute magnetic oxides (DMOs) have attracted significant interest in recent years on account of their potential application in spintronic devices.[1,2] There are numerous reports in the literature that the inclusion of transition metal (TM) dopants leads to ferromagnetism at room temperature, and early work attributed this effect to the $s(p)$-d exchange interaction between the sp band of the host semiconductor and the localized d electrons of the TM ion.[3] However recent work, particularly using x-ray magnetic circular dichroism (XMCD), has indicated that the TM ions are paramagnetic[4,5] and hence do not contribute to the ordered moment. The origin of the ferromagnetism thus remains controversial, with even the necessity for TM doping being called in to question. It has emerged that the most obvious sources for ferromagnetism could be either localized electrons in donor states or free electrons in the conduction band.[6] Coey *et al*. have recently developed a model for defect-related ferromagnetism that involves a spin-split defect band populated by charge transfer from a proximate charge reservoir.[6] In this model, magnetization is limited by defect concentration, not by 3d TM ion doping.

A great many experimental hurdles must be overcome when dealing with DMO materials. A lack of stability and reproducibility halts any concrete conclusions from being made on ferromagnetic behavior. Garcia *et al*. give a full account of the errors that can be encountered when measuring dilute magnetism.[7] Additionally, a comprehensive study by Khalid *et al*. has also shown it is possible to measure very weak ferromagnetic signals from the substrate alone.[8]

Magnetic circular dichroism (MCD) in the optical range is another powerful tool capable of studying spin polarization in the band and defect states associated with the host oxide. This sensitive probe is ideal for exploring the magnetic and electronic properties of DMOs. A measurement of the MCD at photon energy E gives the difference in absorption for left and right circularly polarized light. Therefore, it provides information regarding the way states that participate in the transition at that particular energy are affected by the magnetism. A number of MCD studies have been performed on DMO materials, particularly on ZnO,[9–11] and these have given very useful information concerning the spin polarization of the conduction electrons.

In this paper, we focus on indium oxide (In_2O_3), which is an important functional transparent conducting oxide, especially for the developing field of transparent spintronics.[12] There have been several reports that TM-doped In_2O_3 exhibits ferromagnetism beyond room temperature, and this has sparked interest in its use in spin transport devices.[13–15] We present here an extensive study on Co-doped In_2O_3 thin films, which exhibit room temperature ferromagnetism, grown using dc magnetron sputtering in an oxygen-deficient sputtering ambient. These films have been characterized in detail using x-ray diffraction (XRD), x-ray absorption fine structure (XAFS), along with magnetic and magneto-optical techniques as a function of both the Co concentration, x, and temperature. We find that Co successfully substitutes for In in the In_2O_3 system and that the Co ions are paramagnetic in nature and hence not part of the observed ferromagnetic phase, in agreement with the XMCD data.[5] Furthermore, the magnetization was found to be significantly larger than that which could arise from the free carriers, which leads us to conclude the ferromagnetism is due to localized electrons in donor states. Spectroscopic measurements, especially MCD, indicate that the most likely candidates are the oxygen vacancy levels approximately 0.9 eV below the conduction band. Our results thus explain the previous studies that indicated that oxygen vacancies were essential to ferromagnetism for TM-doped[13–16] and undoped In_2O_3 films.[17]

II. EXPERIMENTAL

A series of five Co-doped In_2O_3 films with Co concentrations ranging from 1.6% to 8.1% were grown using dc magnetron sputtering in a highly oxygen-deficient environment to generate a large density of oxygen vacancies. Pure, undoped In_2O_3 films were also grown under the same conditions as the Co-doped samples and served as a set of control samples. Compositional analysis was performed using energy dispersive x-ray spectroscopy (EDX) using 20×20 μm^2 areas positioned at a number of locations over the sample. The films had thicknesses between 210 and 230 nm and were grown at 300 ° C on (0001) *c*-plane sapphire substrates. The system base pressure was better than 1×10^{-6} Pa. Films were sputtered in 1.2 ± 0.01 Pa of an Ar-O_2 (95:5) mix. Phase identification and structural properties of the Co-doped In_2O_3 were analyzed using XRD on a Bruker diffractometer in the θ-2θ mode using Cu K_α radiation.

The XAFS measurements were performed at beamline 20-ID-B at the Advanced Photon Source using a microfocused beam incident on the sample at approximately 5° glancing angle. The sample was spun about the surface normal to minimize interference from the substrate Bragg peaks. The monochromator used Si (111) crystals, giving an energy resolution of 1 eV. The XAFS signal was detected in fluorescence using a four-element Vortex® detector. Data were collected with the x-ray polarization parallel and perpendicular to the surface. No orientation dependence was found. Because it was of higher quality, the data reported here are for the polarization perpendicular to the surface. Data analysis was carried out using the Athena and Artemis interfaces to the Ifeffit analysis program,[18] and theoretical calculations were made using Feff 8.4.[19]

A superconducting quantum interference device (SQUID) magnetometer was employed for characterization of the bulk magnetic properties. The samples were mounted using a plastic straw fastened with cotton thread. These components were measured alone within the SQUID system and consistently produced a diamagnetic response. Measurements were performed in the temperature range of 5–300 K in magnetic fields up to 1 T. Transport properties were performed through standard four-point measurements in the van der Pauw configuration in the 10–300 K temperature range. Optical absorption and MCD measurements were made with a xenon lamp and monochromator. A photoelastic modulator was used to obtain the MCD as a function of frequency between 1.5 and 3.3 eV. Temperature-dependent MCD spectra in the range 10–300K were taken at 0.5 T in a helium flow cryostat inserted between the poles of an electromagnet. Higher fields, up to 1.8 T, were available for room temperature measurements when the cryostat was removed.

III. RESULTS

A. Structure and composition

EDX analysis revealed that the films were uniformly doped with minimal variation in Co concentration ($\sim \pm 0.15\%$).

Figure 1 shows the θ-2θ XRD scans of Co-doped In_2O_3 films grown on *c*-plane sapphire for a range of Co doping levels. All peaks displayed on the diffractogram could be indexed assuming the same bixbyite cubic structure as pure

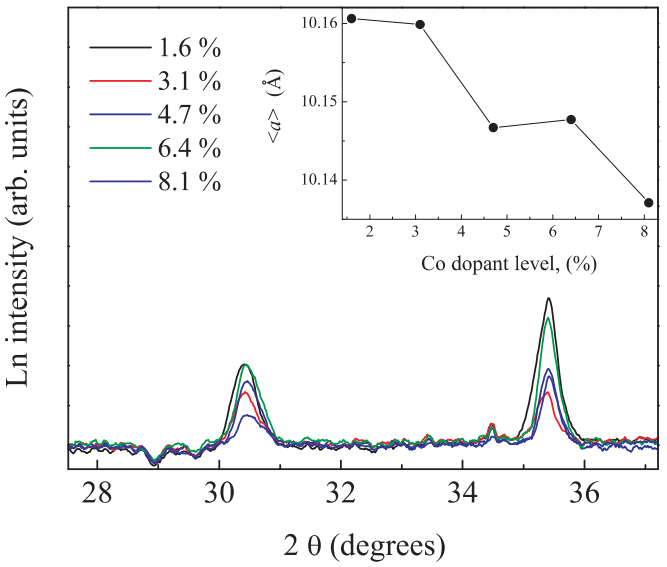

FIG. 1. (Color online) θ-2θ XRD diffractograms focusing on the In_2O_3 (222) and (400) reflection peaks for Co-In_2O_3 films of varying Co concentrations, demonstrating the shift in the peak position upon Co doping. Inset: The steady decrease in the average lattice parameter, *a* (Å), as a function of Co doping.

In_2O_3. The peaks are relatively sharp, indicating that the films have a reasonable degree of crystallinity. At first glance, no detectable peaks corresponding to any secondary Co oxides or Co metal were found. This is often the case in DMOs which appear to be phase pure and of high crystalline quality. Raising the integration time per point to 100 s still gave the same outcome. A shift in the In_2O_3 (222) and (400) diffraction peaks toward higher values of 2θ with increasing levels of Co doping is observed and suggests a gradual decrease in the average out-of-plane lattice parameter, $\langle a \rangle$ (inset, Fig. 1). This is evidence that the smaller Co^{2+} ions (ionic radius 0.74 Å) substitute for the larger In^{3+} ions (ionic radius 0.94 Å) at In sites rather than forming a defect phase.

Figure 2 shows the near-edge XAFS data for the sample with 8.1% Co compared with CoO and Co metal. From

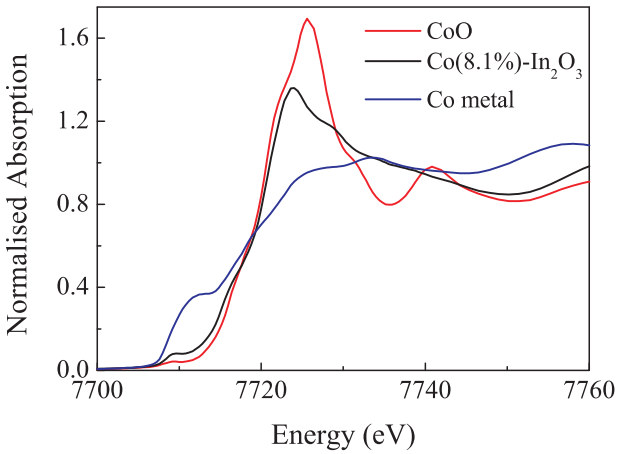

FIG. 2. (Color online) Normalized Co near-edge XAFS spectra for an In_2O_3 sample doped with 8.1% Co compared with CoO and Co metal.

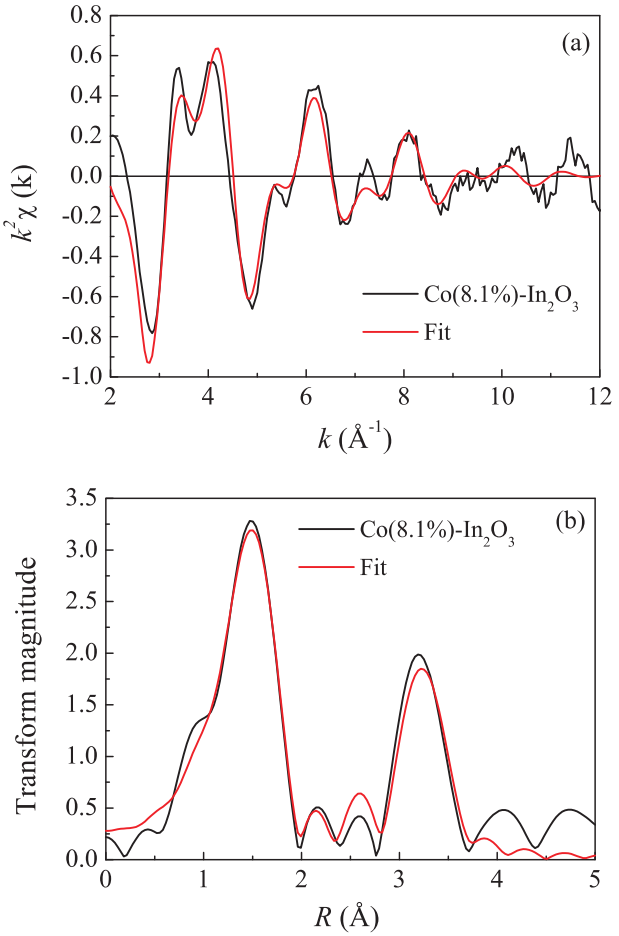

FIG. 3. (Color online) Comparison of the Co EXAFS data for an In_2O_3 sample doped with 8.1% Co compared with a substitutional model fit for the k^2-weighted EXAFS (a) and its Fourier transform (b).

the position of the edges, we can conclude that the Co is predominately Co^{2+}. The increased pre-edge feature near 7710 eV for the sample possibly indicates the presence of a small amount of Co metal. However, the main substitutional site in the bixbyite structure is asymmetric with three different In-O distances in contrast to CoO, which has a symmetric arrangement. Previous results for Co-doped In_2O_3 found a similar increase in the pre-edge region, which was attributed to disorder in the Co site.[20] Asymmetry and disorder tend to increase the magnitude of the pre-edge feature, so we need to look at the extended fine structure (EXAFS) for a more definitive identification of the amount of metal.

The EXAFS data and its Fourier transform are shown in Fig. 3(a) and 3(b), along with fits to the data. The fits were made assuming the Co is substituting into both In sites of the bixbyite structure in the same ratio as their multiplicity (see Table I for a comparison of the two sites). The transform range was $k = 2$–10 Å^{-1} and the R-space data was fit over the range of $R =$ 1–3.7 Å. The EXAFS signal was quite weak, showing a large amount of disorder, but the simple substitutional model fits quite well, with a modest relaxation of the neighboring atoms toward the smaller Co ions. Because the two substitutional sites are quite different, fits were also made assuming the Co

TABLE I. Comparison of the In sites in the bixbyite structure of In_2O_3 used to fit the EXAFS data and its Fourier transform (see Fig. 3). Site 1 is three times more numerous than Site 2. Structure data taken from Ref. 21.

	First Shell	Second Shell	Third Shell
Site 1 (24d)	2 O at 2.04 2 O at 2.14 2 O at 2.41	2 In at 3.34 4 In at 3.35	2 In at 3.84 4 In at 3.85
Site 2 (8a)	6 O at 2.15 Å	6 In at 3.34	6 In at 3.84 6 O at 3.89

preferred a single site. For site 2 (six O at a single distance), the fits were inferior and required an unrealistic reduction in the EXAFS amplitude, whereas for the more disordered and more numerous site 1, the fits were similar in quality to the random case. When Co metal was added to the model, the amount always refined to near zero within experimental error ($\leqslant$2% of the 8.1% of Co doping). Therefore, the XAFS results are consistent with all of the Co substituting into In sites in the $2+$ valence state.

B. Magnetic properties

In-plane magnetization (M) versus applied magnetic field ($\mu_0 H$) measurements displayed clear evidence for ferromagnetism in each of the Co-doped In_2O_3 films up to and above room temperature. The substrates have been repeatedly measured at both low and high temperature and consistently give a diamagnetic response, and the measured ferromagnetic signals are in fact considerably larger than those that have previously been obtained from substrates.[8]

Raw magnetization loops at 5 and 300 K for an 8.1% Co-doped In_2O_3 sample are shown in Fig. 4(a). The raw magnetization was decomposed into two parts: $M = M_1 + M_2$. M_1 varied linearly with the magnetic field (i.e., $M_1 = \chi H$, in the field range of 0.5–1 T), whereas M_2 followed a hysteretic loop. We first consider the linear contribution, M_1. At 300 K the paramagnetic contribution from the film (if present) would have been too small to detect, and the measured value of χ is consistent with the diamagnetic substrate. On cooling to 5 K, a clear positive contribution appeared. Because the susceptibility of the substrate was confirmed to be independent of temperature, we can define $\chi_{\text{film}}(5\text{ K}) = \chi(5\text{ K}) - \chi(300\text{ K})$. The value of $\chi_{\text{film}}(5\text{ K})$, normalized to the film volume, V, is plotted against the Co concentration, x, in Fig. 4(b). The experimental data are compared with the expected susceptibility for paramagnetic Co^{2+} ions, namely $\frac{\chi_{\text{Curie}}}{V} = \frac{N x p_{\text{eff}}^2 \mu_B^2 \mu_0}{3 k_B T}$, where N is the number of In ions (cm^{-3}), x is the cobalt concentration, and $T = 5$ K. The linear variation of χ_{Curie} with x indicates that this additional susceptibility arises from the Co ions. The expected moment is $p_{\text{eff}} = 5$ for Co^{2+} ions[22] in octahedral coordination and takes the spin-only value of $p = 3.87$ for symmetry that is low enough to quench the orbital contribution fully. The agreement with the spin-only value is in agreement with the EXAFS data, which indicates that a high fraction of the Co ions are in sites of low symmetry. This measurement of χ_{Curie}, particularly when taken together with other XMCD data, gives compelling evidence that all of

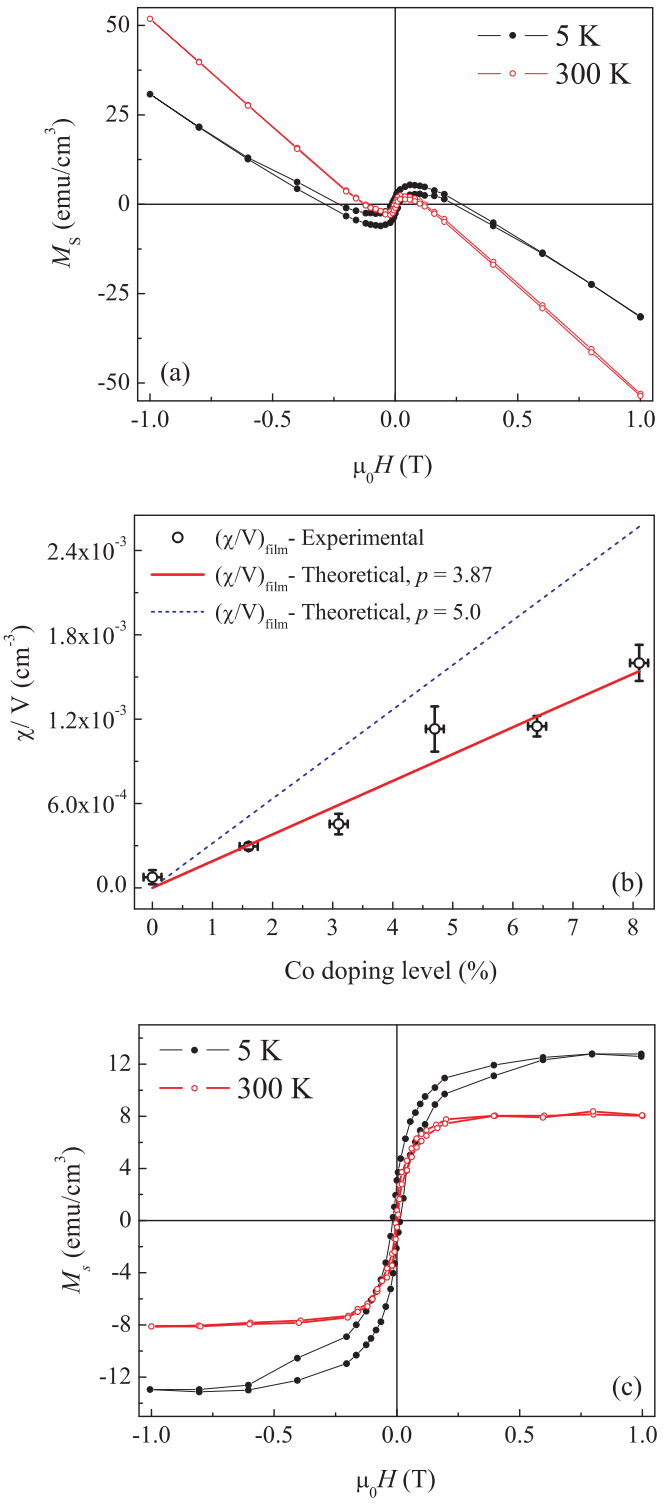

FIG. 4. (Color online) (a) Raw magnetization data for an 8.1% Co-doped In_2O_3 thin film at both 5 K (solid circles) and 300 K (open circles). (b) χ_{film}(5 K), normalized to the film volume, versus the Co concentration, compared with the expected susceptibility of paramagnetic Co^{2+} ions in octahedral coordination. (c) Ferromagnetic hysteresis loops for an 8.1% Co-doped In_2O_3 thin film at both 5 K (solid circles) and 300 K (open circles).

the Co^{2+} ions are paramagnetic and thus do not contribute to the ferromagnetic moment M_2. A similar conclusion was reached from a detailed fit to the low temperature susceptibility of Mn ions in Indium Tin Oxide.[23]

We now consider the ferromagnetic component, M_2. Hysteresis loops for the 8.1% Co sample are shown in Fig. 4(c). The values of the saturated magnetization and coercive fields measured at 300 K and their enhancement on cooling to 5 K for pure and Co-doped In_2O_3 films are given in Table II. This increase in the saturation magnetization is typical for semiconducting samples in which the carrier concentration falls as the temperature is lowered.[13,14] The moment per Co ion at room temperature for the film with highest concentration, 8.1% Co, is 0.38 μ_B/Co which is less than the value of 0.83 μ_B/Co for the film with 1.6% Co, indicating that this magnetism is not due to cobalt clustering (a similar analysis follows if we compare the moments per Co measured at low temperatures). The magnetization recorded for the pure In_2O_3 sample is consistent with zero, although the experimental limit is comparable to the moment observed by Panguluri *et al.*[17] in pure In_2O_3. The values for H_c are similar to those that have been reported for other DMOs[24] and are considerably smaller than those observed at low temperatures if the magnetization is dominated by metallic cobalt.[25]

From $M_S(5)/M_S(300)$ in Table II, we can see that the magnetization in these samples is greatly affected by the changes in temperature, which has been observed before in semiconducting oxide films.[11]

C. Transport properties

Film carrier concentration and mobility were measured to gain insight into the possible mechanisms responsible for magnetism in these samples. These results are summarized in Table II. Results from the Hall measurements indicated that all of the films were found to be *n*-type, as expected for film growth in an oxygen-deficient environment. The resistivities of all the films rose as the temperature was lowered, indicating semiconducting behavior, with the total film resistivity rising with increasing levels of Co doping. Figure 5 shows a typical resistance (R) versus T curve for a Co-doped In_2O_3 film reported in this study. We found a straight line fit for a plot of log R against $T^{-1/4}$ for each of the samples (inset, Fig. 5). The fit was good below 50 K ($= T^*$), but because the fitted values of T_0 (a fitting parameter) ranged between 22 and 31 K, the data failed to satisfy the condition $T^* \ll T_0$ needed for a consistent fit to the variable range hopping theory.[11]

The carrier concentration is reduced for films with 1.6<Co (%)<6.4 compared with a pure In_2O_3 film (4.53×10^{19} cm^{-3}); within this doping range, the carrier concentration is relatively constant, with minimal variation in the saturation magnetization. At 8.1% doping, the carrier concentration has increased and has almost returned to the value of pure In_2O_3; this is accompanied by a sudden rise in the saturation magnetization. Mobility dropped monotonically with doping between 1.6% and 8.1%—from 3.34 cm^2 V^{-1} s^{-1} to 0.95 cm^2 V^{-1} s^{-1}.

The drop in carrier density between the undoped film and the film with 1.6% Co is as one might expect for substituted Co^{2+} ions on In sites acting as acceptors. However, the rest of the samples do not follow this pattern because the carrier

TABLE II. Summary of the magnetization, carrier density, and mobility data for pure and Co-doped In_2O_3 thin films at 5 and 300 K. M_s denotes the saturation magnetization, $\mu_0 H_c$ the coercive field, n_c the free carrier density, and μ_H the carrier mobility.

Co (%)	M_s(300 K) (emu/cm^3)	$\mu_0 H_c$(300 K) (mT)	n_c(300 K) ($\times 10^{19}$cm^{-3})	μ_H(300 K) (cm^2 V^{-1} s^{-1})	M_S(5 K)/ M_S(300 K)	$\mu_0 H_C$(5 K)/ $\mu_0 H_C$(300 K)
0	<0.30	–	4.53 ± 0.12	31.8 ± 0.08	–	–
1.6	3.80 ± 0.10	14.0 ± 0.70	1.89 ± 0.16	3.34 ± 0.18	1.72 ± 0.10	1.01 ± 0.06
3.1	2.59 ± 0.07	21.5 ± 0.90	1.57 ± 0.19	2.88 ± 0.18	1.95 ± 0.06	1.06 ± 0.05
4.7	2.58 ± 0.12	12.4 ± 1.10	1.84 ± 0.17	2.21 ± 0.22	2.14 ± 0.10	1.73 ± 0.20
6.4	6.48 ± 0.30	5.4 ± 0.40	1.87 ± 0.16	2.27 ± 0.20	2.02 ± 0.10	3.52 ± 0.30
8.1	8.75 ± 0.50	3.4 ± 0.30	3.86 ± 0.12	0.95 ± 0.25	1.63 ± 0.09	3.29 ± 0.25

concentration stays approximately constant up to 6.4% and then rises back, almost to the level of pure In_2O_3, at 8.1%. There are many defect states in In_2O_3; the oxygen vacancy states are actually very deep (~0.9 eV below the conduction band) and therefore cannot be responsible for the carriers we observe. The mobile carriers must therefore come from other, shallower, defects. Theory suggests In interstitials either on their own or in combination with an oxygen vacancy.[26] The optical evidence presented in Fig. 6 shows that the Co^{2+} acceptors are taking electrons from the deep donors that do not contribute to the observed carrier density. Hence, we find that the density of mobile carriers measured at room temperature is not linearly dependent on the concentration of Co^{2+} ions, as would be expected for a simple semiconductor.

The total magnetization that can arise from spin-polarized free electrons is $n_c \mu_B$. This is of the order of 0.1 emu/cm^3 for carrier densities of approximately 10^{19} cm^{-3}, which is more than a factor of 10 smaller than the observed magnetization for these samples. We thus deduce that the ferromagnetism cannot be attributed to the free electrons. Given that we have argued above that the ferromagnetism is not due to the Co^{2+} ions either, we therefore need to look at the possible contribution from localized donor states.

A number of studies on doped In_2O_3 have found that the magnetization measured at a given temperature is higher for samples that have been grown more oxygen deficient and have a higher carrier concentration.[13,14] This led to the supposition that a high carrier density is important for magnetism. However, we find here that magnetization increases upon cooling, even though R is rising. Values for n_c for these films were not measured at low temperatures because the resistance was far too high. However, given the R versus T behavior of these samples, we can be fairly certain that n_c falls upon cooling, implying that a greater fraction of the electron carriers are now localized. We see in this study that if the carrier density is reduced by lowering the temperature, the magnetization does not follow the carrier density and in fact does the opposite. This is similar to that reported by Jiang *et al.* for Fe-doped In_2O_3, wherein the magnetization was also found to increase at low temperatures in semiconducting samples.[14] This appears to indicate that the determining feature is the density of defects and not the carrier density itself; the increase in the magnetization at low temperatures, where the carrier density has fallen, may indicate electrons are more magnetic when they are in localized states rather than in extended states.

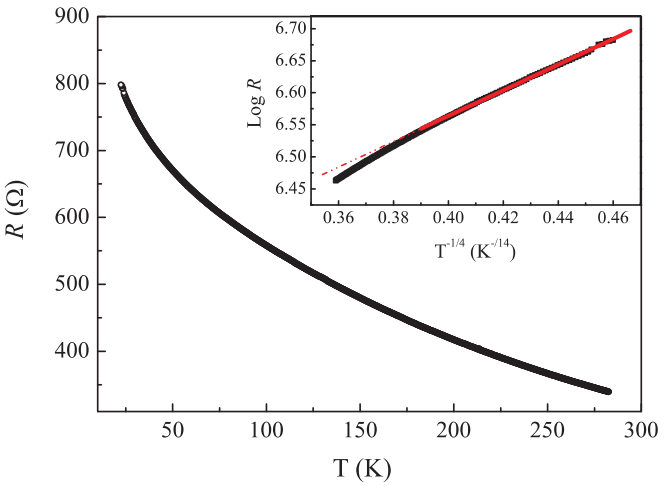

FIG. 5. (Color online) Resistance, R, versus temperature curve for an In_2O_3 film doped with 1.6% Co. Inset: log R versus $T^{-1/4}$ plot for temperatures below 50 K.

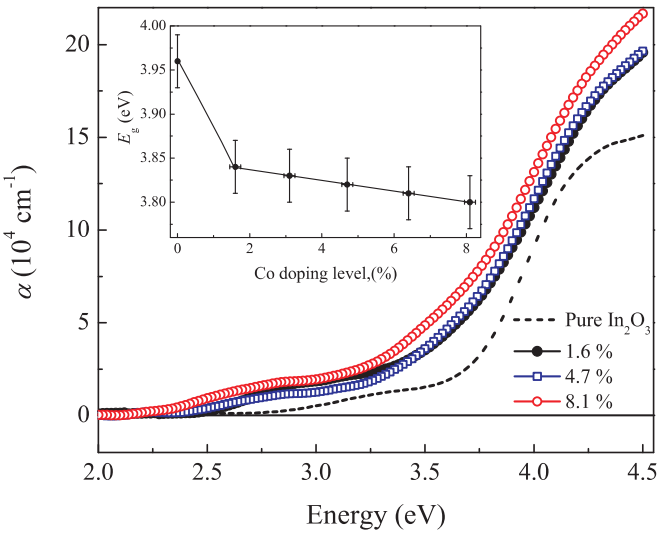

FIG. 6. (Color online) Optical absorption spectra for Co-doped In_2O_3 films with $x = 1.6\%$, 4.7%, and 8.1% at room temperature. The films show the main absorption edge at ~3.4 eV together with an impurity-band shoulder down to ~2.5 eV. Inset: Band gap energy as a function of the Co doping level.

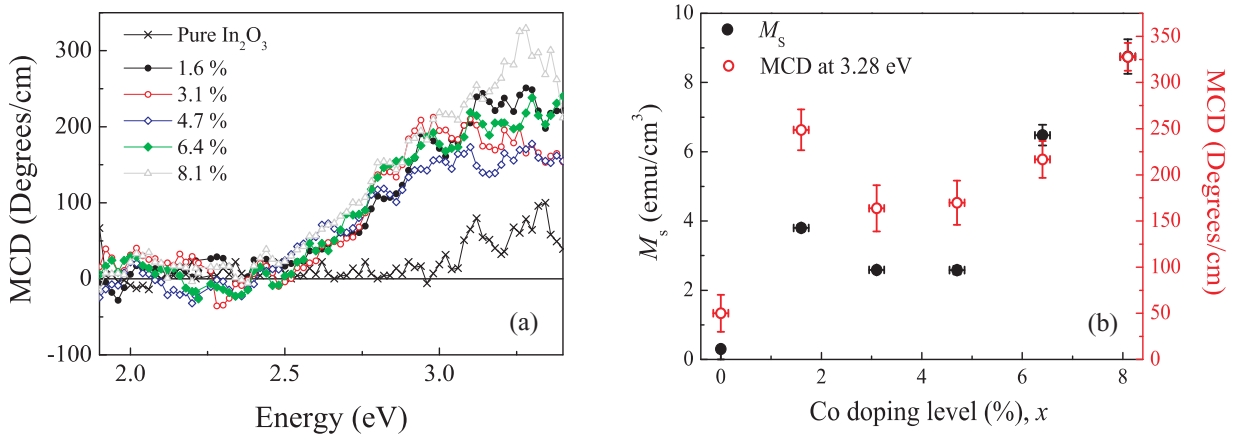

FIG. 7. (Color online) (a) MCD measured at room temperature and 1.8 T for In_2O_3 films with different Co doping levels. (b) Room temperature MCD (taken at 3.28 eV) and saturation magnetization, M_S, as a function of Co doping level. (The scale is chosen so that points superimpose for 8.1%.)

D. Magneto-optical properties

Figure 6 presents optical absorption measurements for pure In_2O_3 and Co-doped In_2O_3, with doping levels of 1.6%, 4.7%, and 8.1%. The band edge of In_2O_3 at 3.4 eV is apparent in each case, together with a shoulder down to 2.5 eV, which is considerably lower than the weak gap transitions seen above 2.9 eV.[27] The shoulders are significantly more pronounced in the Co-doped samples compared with the pure In_2O_3 sample. We attribute this to donor states that have been partially ionized through the compensating effect of the Co^{2+} acceptors substituting for In^{3+}. The donor levels become more pronounced in absorption after doping with Co because more transitions from the valence band to these partially empty states are now possible. The most likely origin of these donor levels is oxygen vacancy states, which have been calculated to lie ~0.9 eV below the band edge.[26] The increasing numbers of allowed transitions from the valence band to the conduction band as a consequence of the broken symmetry introduced by Co doping is also a likely source for the decreasing band gap energy. The inset of Fig. 6 shows the behavior of the band gap energy, E_g, as a function of Co doping. The values for E_g were estimated using Tauc plots, a method that first determines the absorption coefficient, α. Using the relationship $\alpha h\nu \sim (h\nu - E_g)^{1/2}$ and plotting $(\alpha h\nu)^2$ against the photon energy, one can estimate E_g. A sharp decrease is seen upon the initial doping of the In_2O_3 host, after which a much smoother monotonic reduction is observed.

Strong evidence that these donor states are related to the ferromagnetism was obtained by MCD spectroscopy. Figure 7(a) shows the MCD spectra at 300 K and 1.8 T as a function of doping level. The data presented here are the spectra of the films obtained after the MCD of a blank substrate has been subtracted. A clear MCD signal emerges, peaking at the band edge for each of the samples. The magnitude of the MCD is determined both by the strength of the absorption at that energy and the extent to which that state is magnetically polarized. The observation that the MCD is rising for energies above 2.5 eV demonstrates that the transitions that gave rise to the shoulder on the absorption edge involve spin-polarized states. The MCD is significantly lower for the pure In_2O_3 sample compared with the Co-doped samples and is consistent with the very low value of the magnetization and the strength of the shoulders observed in the absorption spectra in Fig. 6. In Fig. 7(b), we show a comparison of the room temperature MCD measured at 3.28 eV with the measured saturation magnetization as a function of the doping. There is a striking similarity between these measurements although the agreement is not fully quantitative.

The origin of the MCD signal was explored in more detail by investigating its temperature dependence. Figure 8 shows the MCD signal at 0.5 T for the 8.1% Co-doped sample from 10 to 300 K. No significant difference is observed at 300 K compared with the 1.8 T measurements in Fig. 7(a), which indicates that the samples are already saturated at 0.5 T, consistent with the magnetization data shown in Fig. 4. The ratio of the magnitude of the MCD at 10 and 300 K agrees very well with the reduction of the magnetization between 5 and 300 K given in Table II. We note that the decrease in magnetization becomes less pronounced as the temperature is raised, unlike that for a localized magnet, in which the reverse is true. The fact that the MCD and the magnetization

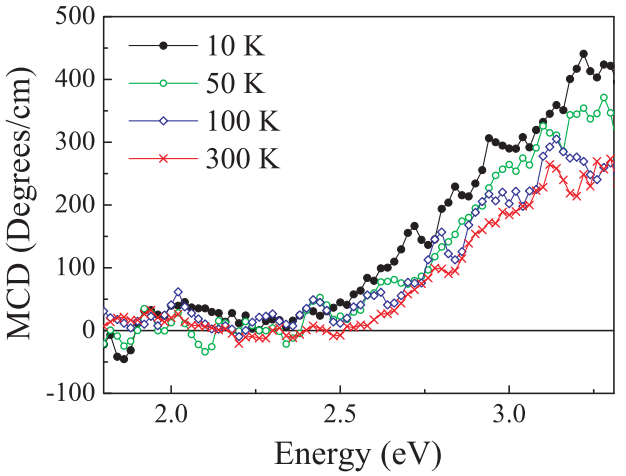

FIG. 8. (Color online) Temperature dependence of the MCD signal for the 8.1% Co-doped In_2O_3 sample measured at 0.5 T.

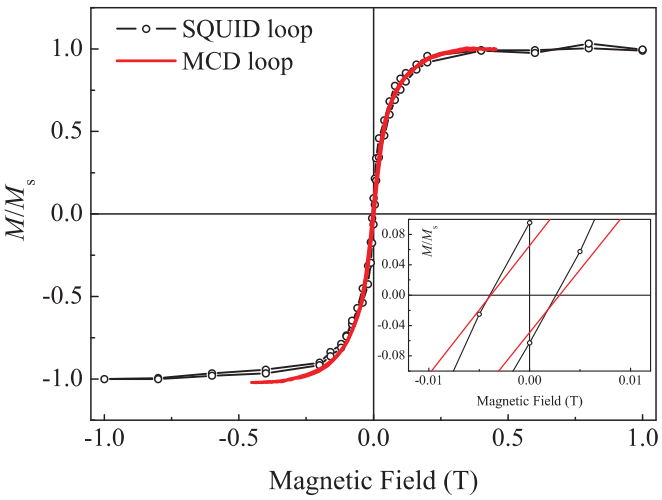

FIG. 9. (Color online) Hysteresis loops for an 8.1% Co-doped In_2O_3 film using a SQUID magnetometer (open circles and line) and using MCD taken at 3.2 eV (solid line) at room temperature. In both cases, the background signal from the substrate was subtracted.

have the same temperature and concentration dependence is strong evidence to support the contention that the observed ferromagnetism originates from the same donor states as those involved in the optical transitions. The ferromagnetic origin of the band edge MCD is confirmed further by the observation of an open MCD hysteresis loop for the Co-doped films. Figure 9 shows such a loop measured at room temperature for an 8.1% Co-doped In_2O_3 sample superimposed upon a magnetic hysteresis loop for the same film measured using a SQUID (data also shown in Fig. 4(c), open circles). The shapes of the loops are very similar, and the coercive fields are almost identical (inset, Fig. 9).

We therefore believe that, in our Co-doped In_2O_3 films, the TM ions are merely acting as acceptors to ionize a larger fraction of the donors and hence produce a partially occupied donor band, as has been suggested theoretically.[6,28] It is this donor band that is responsible for the magnetism. At this stage, we are unable to determine whether the donor states are distributed evenly through the material or concentrated at the grain boundaries, as has been suggested by other studies.[6,29]

IV. SUMMARY AND CONCLUSIONS

We have shown through magnetometry and magneto-optical measurements that semiconducting In_2O_3 is ferromagnetic beyond room temperature both in pure form and when doped using a range of Co content between 1.6% and 8.1%. The Co is found to substitute for In within the In_2O_3 lattice and exists in a Co^{2+} ionic state. Taken together, our data strongly suggest that the magnetism is due to polarized electrons in localized donor states, most probably because of oxygen vacancies. We expect that similar mechanisms might be important in other DMOs.

ACKNOWLEDGMENTS

This research was funded by the U.K. Engineering and Physical Sciences Research Council and KACST (Saudi Arabia). PNC/XSD facilities at the Advanced Photon Source, and research at these facilities, are supported by the U.S. Department of Energy–Basic Energy Sciences, a Major Resources Support grant from NSERC, the University of Washington, Simon Fraser University, and the Advanced Photon Source. Use of the Advanced Photon Source, an Office of Science User Facility operated for the U.S. Department of Energy (DOE) Office of Science by Argonne National Laboratory, was supported by the U.S. DOE under Contract No. DE-AC02-06CH1135. M.S.A. thanks King Saud University, Saudi Arabia, for their kind support.

*alimohakimi@googlemail.com
†g.gehring@sheffield.ac.uk

[1]H. Ohno, Science **281**, 951 (1998).
[2]S. A. Wolf, D. D. Awschalom, R. A. Buhrman, J. M. Duaghton, S. von Molnar, M. L. Roukes, A. Y. Chtchelkanova, and D. M. Treger, Science **294**, 1488 (2001).
[3]T. Dietl, H. Ohno, F. Matsukura, J. Cibert, and D. Ferrand, Science **287**, 1019 (2000).
[4]T. Tietze, M. Gacic, G. Schutz, G. Jakob, S. Bruck, and E. Goering, New J. Phys. **10**, 055009 (2008).
[5]A. M. H. R. Hakimi, F. Schoofs, R. Bali, N. A. Stelmashenko, M. G. Blamire, S. Langridge, S. A. Cavill, G. van der Laan, and S. S. Dhesi, Phys. Rev. B **82**, 144429 (2010).
[6]J. M. D. Coey, P. Stamenov, R. D. Gunning, M. Venkatesan, and K. Paul, New J. Phys. **12**, 053025 (2010).
[7]M. A. Garcia, E. Fernandez Pinel, J. de la Venta, A. Quesada, V. Bouzas, J. F. Fernandez, J. J. Romero, M. S. Martin Gonzalez, and J. L. Costa-Kramer, J. Appl. Phys. **105**, 013925 (2009).
[8]M. Khalid, A. Setzer, M. Ziese, P. Esquinazi, D. Spemann, A. Poppl, and E. Goering, Phys. Rev. B **81**, 214414 (2010).
[9]K. Ando, H. Saito, Z. Jin, T. Fukumura, M. Kawasaki, Y. Matsumoto, and H. Koinuma, Appl. Phys. Lett. **78**, 2700 (2001).
[10]J. R. Neal, A. J. Behan, R. M. Ibrahim, H. J. Blythe, M. Ziese, A. M. Fox, and G. A. Gehring, Phys. Rev. Lett. **96**, 197208 (2006).
[11]A. J. Behan, J. R. Neal, R. M. Ibrahim, A. Mokhtari, M. Ziese, H. J. Blythe, A. M. Fox, and G. A. Gehring, J. Magn. Magn. Mater. **310**, 2158 (2007).
[12]J. W. Seo, J. W. Park, K. S. Lim, J. H. Yang, and S. J. Kang, Appl. Phys. Lett. **93**, 223505 (2008).
[13]F. X. Jiang, X. H. Xu, J. Zhang, X. C. Fan, H. S. Wu, and G. A. Gehring, Appl. Phys. Lett., **96**, 052503 (2010).
[14]F. X. Jiang, X. H. Xu, J. Zhang, X. C. Fan, H. S. Wu, M. Alshammari, Q. Feng, H. J. Blythe, D. S. Score, K. Addison, M. Al-Qahtani, and G. A. Gehring, J. Appl. Phys. **109**, 053907 (2011).
[15]J. Philip, A. Punnoose, B. I. Kim, K. M. Reddy, S. Layne, J. O. Holmes, B. Satpati, P. R. Leclair, T. S. Santos, and J. S. Moodera, Nat. Mater. **5**, 298 (2006).
[16]L. X. Guan, J. G. Tao, C. H. A. Huan, J. L. Kuo, and L. Wang, Appl. Phys. Lett. **95**, 012509 (2009).
[17]R. P. Panguluri, P. Kharel, C. Sudakar, R. Naik, R. Suranarayanan, V. M. Naik, A. G. Petukhov, B. Nadgorny, and G. Lawes, Phys. Rev. B **79**, 165208 (2009).
[18]B. Ravel, and M. Newville, J. Syn. Rad. **12**, 537 (2005).

[19] A. L. Ankudinov, A. I. Nesvizhskii, and J. J. Rehr, Phys. Rev. B **67**, 115120 (2003).
[20] G. Subias, J. Stankiewicz, F. Villuendas, M. P. Lozano, and J. Garcia, Phys. Rev. B **79**, 094118 (2009).
[21] L. V. Morozova, P. A. Tikhonov, and V. B. Glushkova, Inorg. Mater. **27**, 217 (1991).
[22] I. Ardelean, Gh. Ilonca, S. Simon, S. Filip, and T. Jurcut, Mater. Res. Bull. **32**, 191 (1997).
[23] M. Venkatesan, R. D. Gunning, P. Stamenov, and J. M. D. Coey, Appl. Phys. Lett. **103**, 07D135 (2008).
[24] D. A. Schwartz, N. S. Norberg, Q. P. Nguyen, J. M. Parker, and D. R. Gamelin, J. Am. Chem. Soc. **125**, 13205 (2003).
[25] S. M. Heald, T. Kaspar, T. Droubay, V. Shutthanandan, S. Chambers, A. Mokhtari, A. J. Behan, H. J. Blythe, J. R. Neal, A. M. Fox, and G. A. Gehring, Phys. Rev. B **79**, 075202 (2009).
[26] L.-M. Tang, L.-L. Wang, D. Wang, J.-Z. Liu, and K.-Q. Chen, J. Appl Phys. **107**, 083704 (2010).
[27] A. Walsh, J. L. F. Da Silva, S.-H. Wei, C. Korber, A. Klein, L. F. J. Piper, A. DeMasi, K. E. Smith, G. Panaccione, P. Torelli, D. J. Payne, A. Bourlange, and R. G. Egdell, Phys. Rev. Lett. **100**, 167402 (2008).
[28] W. Zhu, X. Qiu, V. Iancu, X.-Q. Chen, H. Pan, W. Wang, N. M. Dimitrijevic, T. Rajh, H. M. Meyer III, M. P., Paranthaman, G. M. Stocks, H. H. Weitering, B. Gu, G. Eres, and Z. Zhang, Phys. Rev. Lett. **103**, 226401 (2009).
[29] B. B. Straumal, A. A. Mazilkin, S. G. Protasova, A. A. Myatiev, P. B. Straumal, G. Schutz, P. A. van Aken, E. Goering, and B. Baretzky, Phys. Rev. B **79**, 205206 (2009).